University of Kentucky
UKnowledge

Anesthesiology Faculty Publications

Anesthesiology

2013

Chiral Polarization Scale of QCD Vacuum and Spontaneous Chiral Symmetry Breaking

Andrei Alexandru
George Washington University

Ivan Horváth
University of Kentucky, horvath@pa.uky.edu

Right click to open a feedback form in a new tab to let us know how this document benefits you.

Follow this and additional works at: https://uknowledge.uky.edu/anesthesiology_facpub

Part of the Anesthesiology Commons

Repository Citation

Chiral Polarization Scale of QCD Vacuum and Spontaneous Chiral Symmetry Breaking

Chiral polarization scale of QCD vacuum and spontaneous chiral symmetry breaking

Chiral polarization scale of QCD vacuum and spontaneous chiral symmetry breaking

Andrei Alexandru[1] **and Ivan Horváth**[2,3]

[1]George Washington University, Washington, DC, USA
[2]University of Kentucky, Lexington, KY, USA

E-mail: `aalexan@gwu.edu, horvath@pa.uky.edu`

Abstract. It has recently been found that dynamics of pure glue QCD supports the low energy band of Dirac modes with local chiral properties qualitatively different from that of a bulk: while bulk modes suppress chirality relative to statistical independence between left and right, the band modes enhance it. The width of such chirally polarized zone – *chiral polarization scale* Λ_{ch} – has been shown to be finite in the continuum limit at fixed physical volume. Here we present evidence that Λ_{ch} remains non–zero also in the infinite volume, and is therefore a dynamical scale in the theory. Our experiments in N_f=2+1 QCD support the proposition that the same holds in the massless limit, connecting Λ_{ch} to spontaneous chiral symmetry breaking. In addition, our results suggest that thermal agitation in quenched QCD destroys both chiral polarization and condensation of Dirac modes at the same temperature $T_{ch} > T_c$.

1. Introduction

The work presented in this talk is part of a long–term effort to look at QCD vacuum structure in a model–independent manner. This involves devising meaningful, preferably gauge invariant, characteristics of gauge configurations dominating QCD path integral. These configurations are accessible via first–principles lattice QCD simulations, and are not altered from their equilibrium form. The underlying assumption is that when objective information of this kind sufficiently accumulates, it can be eventually integrated into a coherent picture of vacuum–related QCD phenomena. This is the *bottom–up approach* to QCD vacuum structure [1].

Our focus here is spontaneous chiral symmetry breaking (SChSB), generally viewed as one of the keys to making sense of low–energy hadronic physics. When thinking about SChSB, Dirac eigenmodes immediately pop out. Indeed, spectral representation turns out to be a fruitful way of looking at $\bar\psi\psi$, revealing that symmetry breakdown is equivalent to Dirac mode condensation. For example, in N_f=2 theory with quark mass m,

$$\lim_{m\to 0}\langle\bar\psi\psi\rangle_m \neq 0 \quad\Longleftrightarrow\quad \lim_{\lambda\to 0}\lim_{m\to 0}\rho(\lambda,m) \neq 0 \tag{1}$$

where $\rho(\lambda,m)$ is the spectral density of modes and we assumed infinite volume [2]. While the above clarifies meaning of chiral symmetry in spectral language, it offers no dynamical detail on the breaking phenomenon. The underlying goal of this project is to identify such detail in local behavior of Dirac modes.
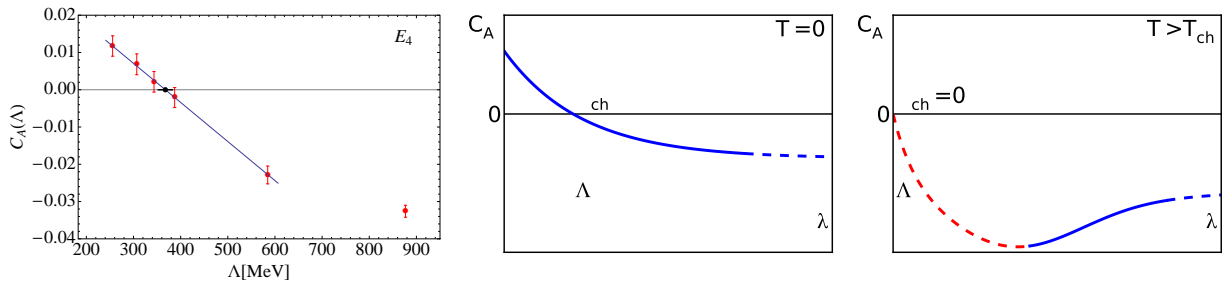
[3] The Speaker.

Figure 1. Left: chiral polarization scale as found in ensemble E_4 of Ref. [4]. Middle: qualitative behavior of $C_A(\lambda)$ in zero–temperature QCD. Right: same after chiral symmetry restoration by thermal agitation.

Our initial interest in this direction are *chiral properties* of the modes, owing to the intuitive expectation that breakdown of chiral symmetry should be imprinted in such features. While global chirality of Dirac non–zeromodes vanishes, the local chiral behavior reflects properties of the underlying gauge background [3]. The simplest "local inquiry" of the above type is whether values $\psi(x) = \psi_L(x) + \psi_R(x)$ tend to appear with equal participation of left/right subspaces or with asymmetric one. In other words, whether they tend to be chirally polarized or anti–polarized. Such questions were asked some time ago with different goals in mind [3], but it turns out that for our purposes it is crucial that the corresponding measures be *dynamical*. In the current context, "dynamical measure" is one that it is uniquely defined and involves comparison to statistical independence of left and right. Such measures have been constructed in Ref. [4].

In this work we will only deal with the most basic polarization measure, namely the correlation coefficient of chiral polarization C_A. This quantifies the overall tendency toward local chiral asymmetry, and is constructed as follows. Consider the probability distribution $\mathcal{P}(\psi_L, \psi_R)$ of left–right components for a mode or some group of modes. Associated with $\mathcal{P}$ is the distribution $\mathcal{P}^u(\psi_L, \psi_R) \equiv P(\psi_L)P(\psi_R)$ describing statistically independent components. Here $P(\psi_L) = \int d\psi_R \mathcal{P}(\psi_L, \psi_R)$ and similarly for $P(\psi_R)$, with functional forms being the same due to the symmetry of $\mathcal{P}$. Now, imagine the experiment in which samples are being drawn simultaneously from $\mathcal{P}$ and $\mathcal{P}_u$, and compared by their polarization. The outcomes of such comparisons have no arbitrariness, and their statistics defines the probability Γ_A that sample chosen from $\mathcal{P}$ is more polarized than one chosen from $\mathcal{P}^u$. The correlation coefficient is then $C_A \equiv 2\Gamma_A - 1 \in [-1, 1]$. Consequently, the dynamics enhancing polarization relative to statistical independence is chirally correlated ($C_A > 0$) while the one suppressing it is anti–correlated ($C_A < 0$): the former supports local chirality while the latter local anti–chirality.

The new dynamical information associated with the above approach is encoded in spectral behavior of $C_A \equiv C_A(\lambda)$, with spectral average in finite volume defined by [5]

$$C_A(\lambda, M, V) \equiv \frac{\sum_k \langle \delta(\lambda - \lambda_k) C_{A,k} \rangle_{M,V}}{\sum_k \langle \delta(\lambda - \lambda_k) \rangle_{M,V}} \tag{2}$$

Here $M \equiv (m_1, m_2, \ldots, m_{N_f})$ is the set of quark masses and $C_{A,k}$ the correlation associated with k-th mode. In Ref. [4] it was found that $C_A(\lambda)$ in quenched QCD has a positive core around zero, and switches to negative values at chiral polarization scale Λ_{ch} (Fig.1, left). It was also shown that Λ_{ch} is non–zero in the continuum limit at fixed physical volume. Here we present evidence that (1) Λ_{ch} remains positive in the infinite volume limit and is thus a dynamical scale in the theory, (2) Λ_{ch} is non–zero in the chiral limit of $N_f = 2 + 1$ QCD and SChSB thus proceeds via chirally polarized modes, and (3) Λ_{ch} vanishes simultaneously with density of near–zeromodes
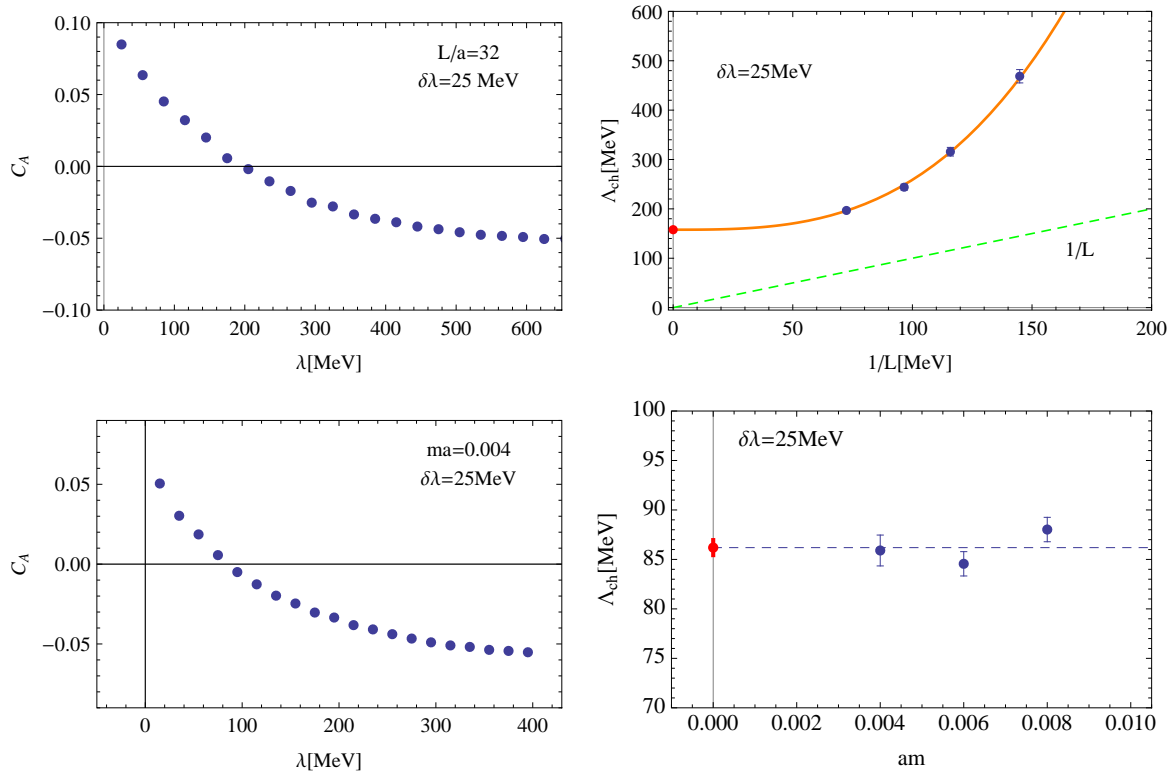
Figure 2. Top: $C_A(\lambda)$ for $L = 32$ lattice of quenched QCD (left) and infinite volume extrapolation (right). Bottom: $C_A(\lambda)$ for m_l=0.004 lattice of N_f=2+1 QCD (left) and chiral limit extrapolation (right).

when temperature is turned on, and is thus a scale closely tied to SChSB. Qualitative behavior of $C_A(\lambda)$ in zero–temperature QCD is shown in the middle plot of Fig.1, while that in the chirally symmetric phase at finite temperature is on the right.

2. Infinite volume and chiral limit.

We start with the question of infinite volume limit. As pointed out in Ref. [4], this is of crucial importance in order to establish that Λ_{ch} represents dynamically generated scale of QCD. We perform the volume study in the context of pure glue lattice QCD with Wilson action at fixed gauge coupling β=6.054. Using the parametrization of Ref. [6] and value r_0=0.5 fm this translates into the lattice spacing a=0.085 fm. Lattices of sizes 16^4, 20^4, 24^4 and 32^4 were studied with 100 independent configurations generated in each case.

To probe local chiral properties of modes, we use overlap Dirac operator with parameters $r=1$ and $\rho=26/19$, and these settings were used throughout this study. Approximately 200 conjugate pairs of lowest near–zeromodes were computed on each configuration, and the average $C_A(\lambda)$ was determined in the available region of the spectrum. In Fig.2 (top left) we show the result for the largest volume, exhibiting the anticipated behavior, and with clearly defined chiral polarization scale. Dependence of Λ_{ch} on the infrared cutoff is shown in the top right plot of Fig.2, together with the cutoff $1/L$ itself. The data clearly curves away from the cutoff, indicating a positive infinite volume limit. The fit of the form $\Lambda_{ch}(1/L) = \Lambda_{ch}(0) + b\,(1/L)^3$ was used to extrapolate to infinite volume, yielding $\Lambda_{ch} \approx 160$ MeV at this cutoff. Judging by the behavior of continuum extrapolation in Ref. [4], the continuum limit is estimated to be $\Lambda_{ch} \approx 150$ MeV in Wilson regularization of quenched QCD.
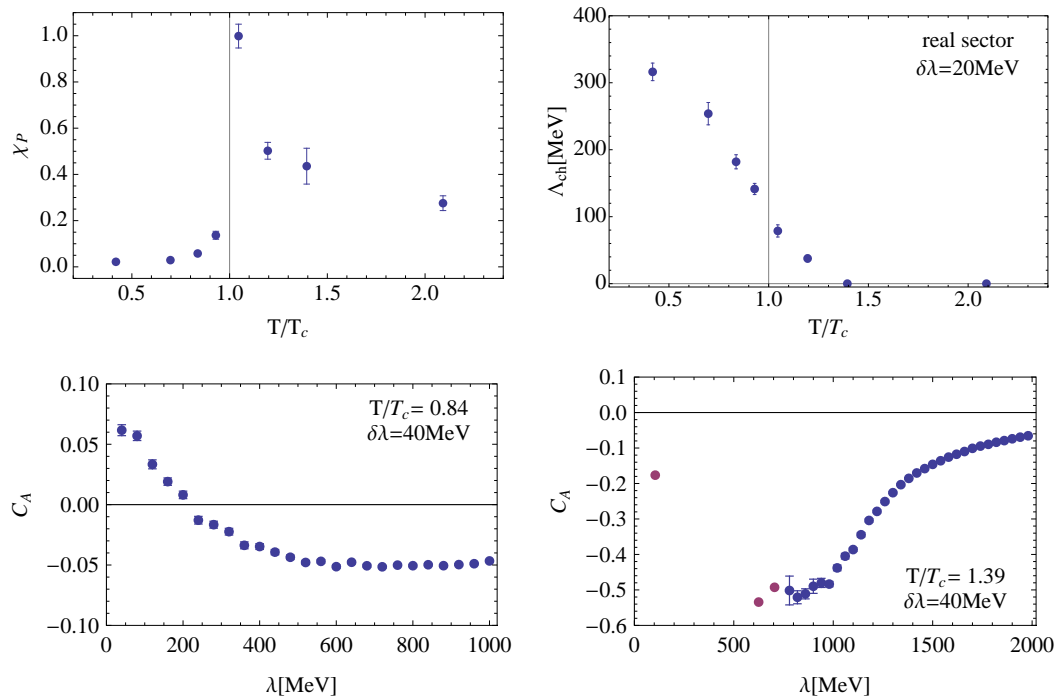
Figure 3. Top: temperature dependence of Polyakov line susceptibility (left) and chiral polarization scale (right) as discussed in the text. Bottom: behavior of $C_A(\lambda)$ at $T/T_c = 0.84$ (left), and at $T/T_c = 1.39$ (right).

To study the effects of dynamical fermions, we use the $N_f=2+1$ **RBC/UKQCD** domain wall fermion ensembles of Ref. [7]. These $32^3 \times 64$ lattices are at fixed heavy bare mass $m_h a = 0.03$, approximately corresponding to mass of physical strange quark, and at fixed lattice cutoff $a = 0.085$ fm. The light quark masses $m_l a = 0.004, 0.006, 0.008$ reach the lightest pion mass of 295 MeV. Low–lying overlap Dirac eigenmodes were computed on 50 configurations from each ensemble, with functions $C_A(\lambda)$ evaluated on the spectral region available. The result for lightest quark mass is displayed on the bottom left plot of Fig. 2, showing behavior qualitatively similar to quenched case. Chiral polarization scale has been reduced due to the effects of light dynamical quarks, but the sensitivity to light mass has already become negligible in this region, as seen on the bottom right plot of Fig. 2. Positive chiral limit, indicated via extrapolation by a constant, is thus expected. The preferred value is $\Lambda_{ch} \approx 86$ MeV at this cutoff, with rough estimate of $\Lambda_{ch} \approx 80$ MeV in the continuum. Note that, due to flat mass dependence, the above estimates apply both at physical point and in the chiral limit.

3. Chiral transition

We now wish to examine whether low–energy chiral polarization could be tied to chiral symmetry breaking in yet more fundamental way. In particular, we study whether the condensation of Dirac modes ($\rho(\lambda \to 0) > 0$) and chiral polarization ($\Lambda_{ch} > 0$) tend to occur simultaneously [5]. To that end, we consider quenched QCD at finite temperature T where it is expected that, for $T > T_{ch}$, Dirac modes cease to condense, and "valence" chiral symmetry becomes restored. Note that the chiral transition temperature was denoted as T_{ch}, in order to distinguish it from the deconfinement temperature T_c defined by the breakdown of Z_3 symmetry.

We use Wilson lattice regularization again, at the identical gauge coupling $\beta=6.054$. Overlap Dirac eigenmodes were computed on $20^3 \times N_t$ lattices with $N_t = 20, 12, 10, 9, 8, 7, 6, 4$, spanning
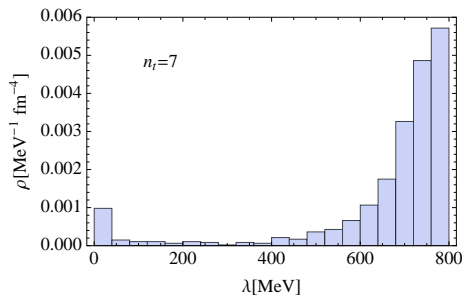
Figure 4. Detail of mode density at low end of the spectrum for N_t=7. Isolated band of near–zero modes is clearly visible. Zero modes are not included.

both confined and deconfined regions. In the top left panel of Fig. 3 we plot the temperature dependence of Polyakov line susceptibility, showing expected behavior with peak at $T/T_c = 1.05$ (N_t=8). The value of T_c, including all extrapolations, is taken from Ref. [8]. Note that for spectral calculations, only configurations from the "real Z_3" Polyakov line sector were used [9], so that the continuation to theory with dynamical quarks is smooth.

In Fig. 3 (bottom) we show the computed $C_A(\lambda)$ at T/T_c=0.84 (N_t=10), and at T/T_c=1.39 ($N_t = 6$). In the former (confined) case there is a positive core of chiral polarization, while only anti–polarization exists in the (deconfined) latter.[4] Closer inspection reveals a discrepancy of chiral polarization behavior with respect to confinement, but not with respect to mode condensation. Indeed, as can be seen in Fig. 3 (top right), chiral polarization is present ($\Lambda_{ch} > 0$) at T/T_c=1.2 ($N_t = 7$), i.e. quite safely in the deconfined phase. At the same time though, as the profile of mode density in Fig. 4 suggests, $\rho(\lambda) > 0$ in the narrow band close to zero, consistently with condensation and breakdown of valence chiral symmetry. The residual density of this kind was first observed in [10]. Our result thus supports both the polarization–condensation equivalence conjecture of Ref. [5], and the possibility that $T_{ch} > T_c$ in quenched QCD.

4. Discussion

"Bottom–up" approach to QCD vacuum structure starts with identifying the features associated with important vacuum effects, such as confinement or SChSB, and characterizing them in a model–independent manner. Here we focused on SChSB and found that it is intimately tied to *dynamical local chirality* of low–lying Dirac modes. In particular, strong interaction supports the band of chirally polarized low–energy modes that condense, and are thus "carriers" of the breaking phenomenon. The width of the band Λ_{ch} provides for a new dynamical scale associated with SChSB. Simultaneous occurrence of mode condensation and chiral polarization at finite temperature supports the possibility that chiral symmetry breakdown (true and "valence") is equivalent to presence of chiral polarization, and thus non–zero Λ_{ch} [5]. This would extend the equivalence of Eq. (1) to include the independent condition $\lim_{m \to 0} \Lambda_{ch}(m) > 0$.

References

[1] Horváth I 2006 *Preprint* `hep-lat/0605008`
[2] Banks T and Casher A 1980 *Nucl.Phys.* **B169** 125 (*Preprint* `hep-lat/9501037`)
[3] Horváth I, Isgur N, McCune J, Thacker H B 2002 *Phys.Rev.* **D65** 014502 (*Preprint* `hep-lat/0102003`)
[4] Alexandru A, Draper T, Horváth I, Streuer T 2011 *Annals Phys.* **326** 1941 (*Preprint* `arXiv:1009.4451`)
[5] Alexandru A and Horváth I 2012 *Preprint* `arXiv:1210.7849`
[6] **ALPHA** Collaboration, Guagnelli M, Sommer R and Wittig H 1998 *Nucl.Phys.* **B535** 389 (*Preprint* `hep-lat/9806005`)
[7] **RBC** and **UKQCD** Collaborations, Mawhinney R 2009 *PoS* **LAT2009** 81 (*Preprint* `arXiv:0910.3194`)
[8] Karsch F 1998 *Nucl. Phys. Proc. Suppl.* **60A** 169 (*Preprint* `hep-lat/9706006`)
[9] Chandrasekharan S and Christ N 1996 *Nucl. Phys. Proc. Suppl.* **47** 527 (*Preprint* `hep-lat/9509095`)
[10] Edwards R G, Heller U M, Kiskis J E, Narayanan R 2000 *Phys.Rev.* **D61** 074504 (*Preprint* `hep-lat/9910041`)

---

[4] The red points in the plot for $T/T_c = 1.39$ denote bins with not enough eigenmodes for error to be estimated.